JOURNAL OF MATERIALS SCIENCE **39** (2004) 1429– 1432

Size-controlled polyelectrolyte nanocapsules via layer-by-layer self-assembly

H. AI, J. GAO
Department of Biomedical Engineering, Case Western Reserve University, Cleveland, OH 44106
E-mail: jinming@cwru.edu

Nanomaterials have found many important applications in biomedical, pharmaceutical, electronic, and molecular diagnostic fields. The recent introduction of electrostatic layer-by-layer (LbL) self-assembly technique enables the design and development of polymer/polymer and polymer/nanoparticle complexes at nanometer scale [1]. The LbL technique is based on alternate adsorption of oppositely charged materials, mostly linear polyelectrolytes, via electrostatic interactions. Multilayer ultrathin films can be developed with "molecular architecture" design with precise control of thickness and molecular composition [2]. This technique has been widely used to coat thin films on two-dimensional substrates [1–4]. In addition, the assembly of multilayers of charged materials has also been applied onto micro/nano-templates including colloidal particles [5, 6], biological cells [7], and drug microcrystals [8, 9].

Among various LbL self-assembled structures, hollow polyelectrolyte capsules are of special interests as a platform device for applications in drug delivery, bioreactor design and biosensing. These polyelectrolyte capsules have several unique characteristics over conventional capsules (e.g. liposomes). First, different materials, including charged polymers, enzymes, inorganic nanoparticles, and antibodies, can be incorporated during capsule formation. Second, capsule wall thickness can be accurately controlled from 5 to 50 nm with a precision less than 1 nm [2]. Third, the polyelectrolyte capsules can shift from an "open" to a "closed" state or vice versa by changes in environmental conditions such as temperature [10], pH [11, 12], or presence of organic solvents [13]. This unique feature permits the efficient loading of molecules inside the hollow capsules [11, 14]. Up to now, hollow polyelectrolyte capsules have been reported at sizes greater than one micron [5, 10–13]. This size limitation is due to the lack of the nano-sized weakly crosslinked melamine formaldehyde (MF) colloidal particles as decomposable core templates during capsule formation [5, 10–13]. In this study, we describe a convenient procedure to produce monodisperse, nanosized MF particles and subsequent nano-sized polyelectrolyte capsules with an accurate control of capsule size.

First, we developed a surface erosion procedure to fabricate MF nanoparticles in precisely controlled acidic pH solutions. It was reported that complete MF particle decomposition was achieved after 20 s in a pH 1.1 HCl solution [17]. Here, we use higher pH (>1.9) to reduce particle size through partial degradation. In a typical experiment, monodisperse 1.2 μm MF particles (Microparticles GmbH, Germany) were suspended in acidic HCl solutions (6×10^5 particles/mL) with a specific pH value from 1.9 to 2.2. At different times, particle suspensions were analyzed by dynamic light scattering (DLS) (90Plus Submicron Particle Size Analyzer, Brookhaven Instruments) to measure the particle diameters in solution at room temperature. Particle surface charge before and after treatment was also characterized by zeta-potential measurement in 1 mM KCl solution.

Fig. 1 shows the particle diameter as a function of decomposition time at pH values 1.9, 2.0, and 2.2. The original MF particle size was characterized as 1279 ± 79 nm from DLS study. After 60 min, a particle diameter of 222 ± 11 nm was obtained in pH 1.9 solution. Treatment in pH 2.0 and 2.2 HCl solutions for 60 min led to particle diameters of 415 ± 30 and 702 ± 11 nm, respectively. Decomposition kinetics at these pH values clearly deviates from the previous observation of linear size reduction over time at pH 1.1 [17]. In this study, a dramatic particle size decrease in the first 20 min was observed in all of the HCl solutions. More specifically, particle size decreased from 1279 ± 79 nm to 826 ± 18 nm, 509 ± 31 nm, and 273 ± 19 nm after 20 min hydrolysis in pH 2.2, 2.0, and 1.9 solutions, respectively. These sizes correspond to 69%, 42%, and 23% of the original particle diameter. Between 20 and 60 min, the particle size decreased more slowly with less than 20% size reduction. Logarithmic curve fitting (KaleidaGraph, version 3.06) provides a reasonable approximation of the experimental decomposition kinetics (Fig. 1). Current work is in progress to investigate the mechanism of polymer hydrolysis at different pH values and the resulting size reduction of weakly crosslinked MF particles. The data in Fig. 1 demonstrate that particle diameter depends on both hydrolysis time and pH values. Prolonged acid treatment (>20 min) at precisely controlled pH values should provide the best strategy in the reproducible control of particle sizes. It also should be noted that acid-hydrolyzed MF particles are positively charged and have similar zeta-potential (e.g. the zeta-potential for the 373 nm MF particles is 28.7 ± 6.3 mV, $n = 3$) to the unmodified MF particles (29.4 ± 3.5 mV, $n = 3$).

We used scanning electron microscopy (SEM, Hitachi S-4500 model) to further characterize the particle size and surface morphology. Fig. 2 shows the SEM

0022–2461

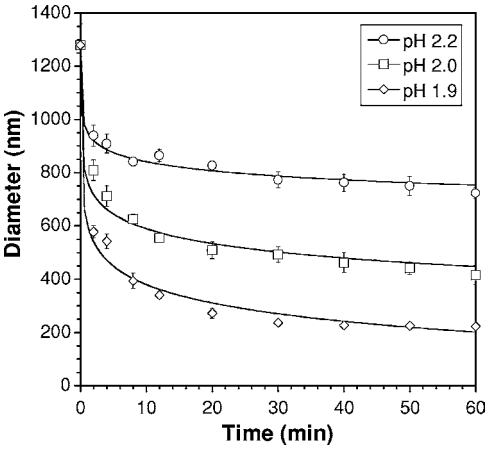

Figure 1 Diameters of MF particles as a function of hydrolysis time at different pH values. All data points were measured by DLS ($n = 5$). Particle size was reduced to 702 ± 11, 415 ± 30 and 222 ± 11 nm after 60 min hydrolysis in pH 2.2, 2.0 and 1.9 HCl solutions, respectively. Logarithmic curve fitting was performed to fit the experimental data.

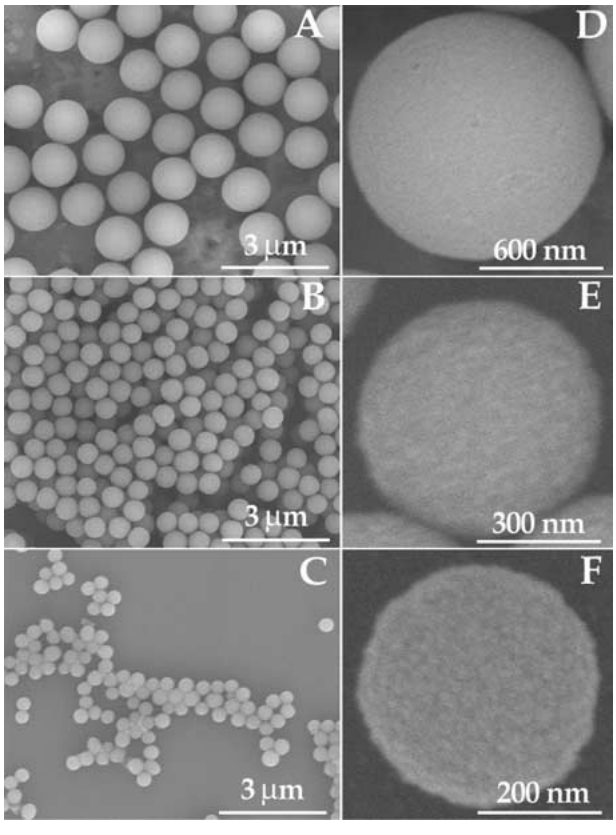

Figure 2 SEM images of MF particles before hydrolysis (A, D) and 8 (B, E) and 60 min (C, F) after hydrolysis in pH 2.0 HCl solution. The average particle diameters are 1183 ± 25, 597 ± 15 and 373 ± 18 nm in A, B and C, respectively. Figs D, E, and F show the amplified individual MF particles from A, B, and C, respectively.

images of MF particles before hydrolysis, 8 and 60 min after hydrolysis in pH 2.0 HCl solution. SEM image of the original MF particles confirms the monodisperse distribution of these particles (Fig. 2A). The particle diameter from SEM analysis is 1183 ± 25 nm, which is slightly smaller than the DLS measurement (1279 ± 79 nm). At higher magnification ($\times 25$ K), the original MF particles are clearly shown in a spherical shape with a smooth surface (Fig. 2D). Figs 2B and C demonstrate that MF particles mostly maintained the spherical shape and monodisperse size distribution after 8 and 60 min hydrolysis, respectively. In addition, the relatively smooth surface morphology of acid-hydrolyzed MF particles (Fig. 2E and F) indicates a surface-erosion mechanism for the particle decomposition. Based on the above SEM images, we measured the particle diameters as 597 ± 15 and 373 ± 18 nm for MF particles after 8 and 60 min hydrolysis, respectively. These values are slightly lower than those measured by dynamic light scattering (650 ± 20 and 430 ± 30 nm after 8 and 60 min hydrolysis, respectively). The smaller particle diameter by SEM analysis most likely reflects the particle shrinkage due to dehydration during sample preparation for SEM analysis.

Next, we used LbL self-assembly technique to coat charged polymers onto the nano-sized MF particles. Gelatin is a denatured form of collagen and is widely used in pharmaceutical applications. Capsules composed of gelatin multilayers effectively sustain the drug release half-life over 300 times [8]. Here we chose negatively charged gelatin (MW = 50 kD, Sigma) as a key component for the capsule formation in this study. Typically, MF particles were first suspended in 2 mg/mL gelatin solution in pH 7.4 PBS for 30 min. Centrifugation was used to remove excess polymer before coating the next layer. A second layer of poly(dimethyldiallyl ammonium chloride) (PDDA, MW = 200 kD, Polysciences) was applied following a similar coating procedure. In total, five bilayers of gelatin and PDDA were introduced to the MF particle surface. Subsequently, core decomposition was carried out in a pH 1.2 HCl solution for 2 min followed by removal of degraded MF oligomers. Hollow polyelectrolyte nanocapsules composed of $(\text{gelatin/PDDA})_5$ were thus obtained. It should be noted that choosing appropriate pH during assembly is important to maintain a high degree of ionization for the oppositely charged polymers. Gelatin is a protein-based zwitterionic molecule with an isoelectric point of 4.5. Carboxylic acids (pKa 3.9–4.5) [18] on the side chains of Glu and Asp residues contribute to the negative charges of gelatin. Sufficiently high pH values (e.g. pH 7.4 in this study) are necessary to fully deprotonate these charged groups and maintain the polyanionic state of the molecule for LbL self-assembly.

Fig. 3 shows the SEM images of three sets of polyelectrolyte capsules using MF particles (Fig. 2) as core templates. Because the inner MF cores were completely decomposed and dissolved, SEM images demonstrated a collapsed shell structure as a result of sample dehydration. Hollow shells appeared to be slightly larger than the core templates although these differences were not statistically significant. The average diameters were 1224 ± 85, 627 ± 32 and 392 ± 19 nm for shells assembled on core templates of 1183 ± 25, 597 ± 15 and 373 ± 18 nm in diameters, respectively. Fig. 3B and C inserts further show the magnified SEM images of individual nanocapsules. Wrinkled edges were clearly present at the boundary of nanocapsules. The flat capsule interior confirmed the complete core decomposition and dissolution. These data further demonstrate the capsule stability following the sample drying process,

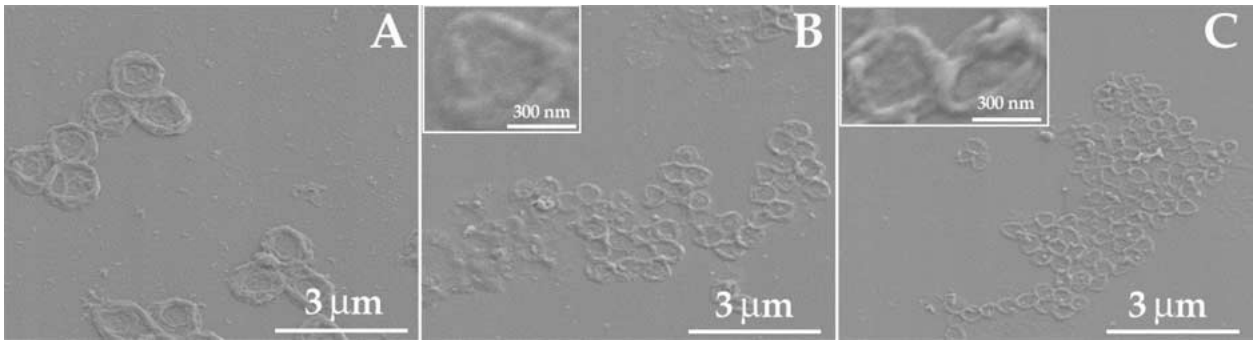

Figure 3 SEM images of hollow polyelectrolyte capsules composed of five bilayers of (gelatin/PDDA). Capsules in A, B, and C were produced using MF particles of 1183, 597 and 373 nm in diameter as core templates (Fig. 2), respectively. Corresponding capsule sizes were achieved at 1224 ± 85 (A), 627 ± 32 (B), and 392 ± 19 nm (C).

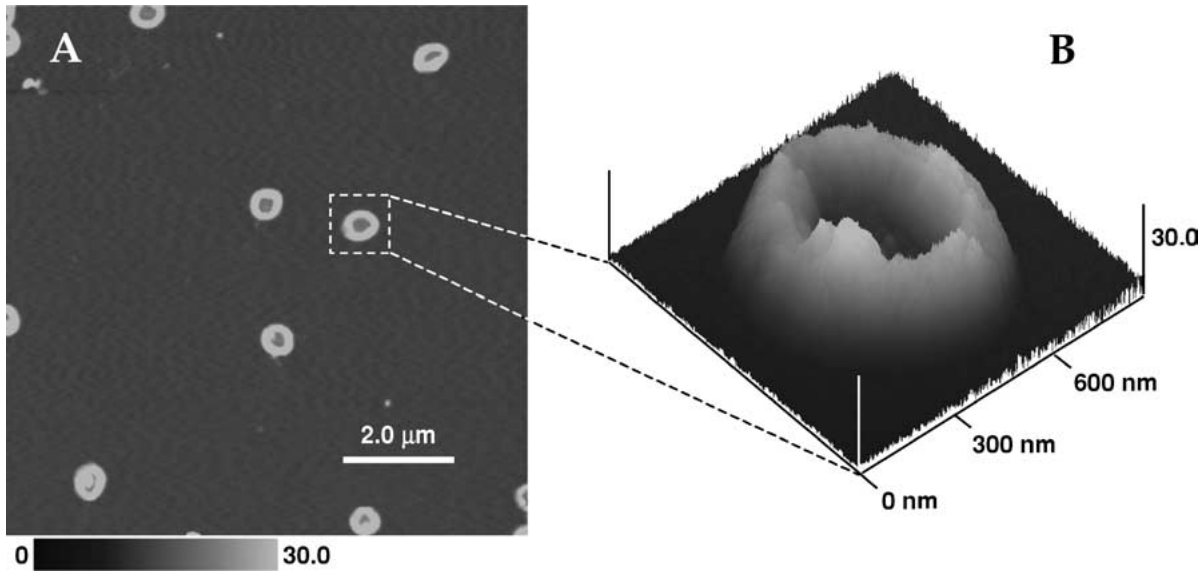

Figure 4 SFM images of 620 nm nanocapsules. (A) Lower magnification image shows the nanocapsules of ring shapes with a relatively uniform size distribution. (B) Three-dimensional image of a single nanocapsule with a boundary thickness of approximately 30 nm.

which is probably a unique attribute to the electrostatic interactions between the oppositely charged layers.

To validate the SEM data, we also examined the nanocapsules by scanning force microscopy (SFM) using a Nanoscope III Multimode SFM (Digital Instrument Inc., Santa Barbara, CA). Silicon tips (Nanosensors, Germany) with a resonance frequency of ~330 kHzand a spring constant of ~40 N/m were utilized for tapping mode imaging. Fig. 4A shows the SFM images of multiple nanocapsules with an average diameter of 636 ± 28 nm (same batch of sample as in Fig. 3B), which is consistent with the SEM measurement (627 ± 32 nm). Moreover, SFM images also showed a uniform size distribution of polymer nanoshells with collapsed shell morphology. Fig. 4B shows an individual nanoshell in 3-dimensions. The nanoshell is ring shaped and the height of polymer folds at the shell boundary was measured to be approximately 30 nm.

In conclusion, we report the successful development of monodisperse MF nanoparticles from 200 to 900 nm using a convenient surface erosion procedure. These MF particles permit the successful development of hollow polyelectrolyte nanocapsules by the LbL self-assembly technique. The procedure allows the accurate control of size, membrane composition and thickness of the nanocapsules. The unique and versatile design of the nanocapsule structure and compositions will potentially open up many opportunities in biomedical and pharmaceutical applications.

Acknowledgment

We thank Dr. Steven Eppell and Dr. Brian Todd for their help on SFM analysis of nanocapsules. This research is supported by an NIH grant (CA 93993).

References

1. G. DECHER, *Science* **227** (1997) 1232.
2. Y. LVOV and H. MÖHWALD, "Protein Architecture: Interfacial Molecular Assembly and Immobilization Biotechnology" (M. Dekker Publ., New York, 2000) p. 125.
3. D. ELBERT, C. HERBERT and J. HUBBELL, *Langmuir* **15** (1999) 5355.
4. P. HO, J. KIM, J. BURROUGHES, H. BECKER, S. LI, T. BROWN, F. CACIALLI and R. FRIEND, *Nature* **404** (2000) 481.
5. E. DONATH, G. SUKHORUKOV, F. CARUSO, S. DAVIS and H. MÖHWALD, *Angew. Chem. Int. Ed.* **37** (1998) 2201.

6. M. FANG, P. GRANT, M. MCSHANE, G. SUKHORUKOV, V. GOLUB and Y. LVOV, *Langmuir* **18** (2002) 6338.
7. H. AI, M. FANG, S. JONES and Y. LVOV, *Biomacromolecules* **3** (2002) 560.
8. H. AI, S. JONES, M. DE VILLIERS and Y. LVOV, *J. Control. Release* **86** (2003) 59.
9. X. QIU, S. LEPORATTI, E. DONATH and H. MÖHWALD, *Langmuir* **17** (2001) 5375.
10. G. IBARZ, L. DAHNE, E. DONATH and H. MÖHWALD, *Chem. Mater.* **14** (2002) 4059.
11. G. SUKHORUKOV, A. ANTIPOV, A. VOIGT, E. DONATH and H. MÖHWALD, *Macromol. Rapid. Commun.* **22** (2001) 44.
12. O. TIOURINA, A. ANTIPOV, G. SUKHORUKOV, N. LARIONOVA, Y. LVOV and H. MÖHWALD, *Macromol. Biosci.* **1** (2001) 209.
13. Y. LVOV, A. ANTIPOV, A. MAMEDOV, H. MÖHWALD and G. SUKHORUKOV, *Nano Lett.* **1** (2001) 125.
14. H. AI, V. SHETH, A. WIEDMANN, D. SUTTON and J. GAO, in "Transactions of the 29th Society for Biomaterials Annual Meeting" (Reno, Nevada, 2003, abstract No. 149).
15. D. LAVAN, D. LYNN and R. LANGER, *Nat. Rev. Drug. Discov.* **1** (2002) 77.
16. Y. WANG, S. HUSSAIN and G. KRESTIN, *Eur. Radiol.* **11** (2001) 2319.
17. C. GAO, S. MOYA, H. LICHTENFELD, A. CASOLI, H. FIEDLER, E. DONATH and H. MÖHWALD, *Macromol. Mater. Eng.* **286** (2001) 355.
18. T. CREIGHTON, in "Proteins Structures and Molecular Properties" (W. H. Freeman and Company, New York, 1993) p. 6.

Received 17 June
and accepted 16 September 2003